

# Evidence for weak interaction between phytochromes Agp1 and Agp2 from *Agrobacterium fabrum*

Peng Xue<sup>1</sup>, Afaf El Kurdi<sup>1</sup>, Anja Kohler<sup>1</sup>, Hongju Ma<sup>1</sup>, Gero Kaeser<sup>1</sup>, Arin Ali<sup>2</sup>, Reinhard Fischer<sup>2</sup>, Norbert Krauß<sup>1</sup> and Tilman Lamparter<sup>1</sup>

<sup>1</sup> Botanical Institute, Karlsruhe Institute of Technology, Germany

<sup>2</sup> Institute for Applied Biosciences, Karlsruhe Institute of Technology, Germany

## Correspondence

T. Lamparter, Botanical Institute, Karlsruhe Institute of Technology, 76131 Karlsruhe, Germany

Tel: +49 (0)721 608 45441

E-mail: tilman.lamparter@kit.edu

(Received 21 December 2018, revised 25 March 2019, accepted 28 March 2019)

doi:10.1002/1873-3468.13376

Edited by Miguel De la Rosa

During bacterial conjugation, plasmid DNA is transferred from cell to cell. In *Agrobacterium fabrum*, conjugation is regulated by the phytochrome photoreceptors Agp1 and Agp2. Both contribute equally to this regulation. Agp1 and Agp2 are histidine kinases, but, for Agp2, we found no autophosphorylation activity. A clear autophosphorylation signal, however, was obtained with mutants in which the phosphoaccepting Asp of the C-terminal response regulator domain is replaced. Thus, the Agp2 histidine kinase differs from the classical transphosphorylation pattern. We performed size exclusion, photoconversion, dark reversion, autophosphorylation, chromophore assembly kinetics and fluorescence resonance energy transfer measurements on mixed Agp1/Agp2 samples. These assays pointed to an interaction between both proteins. This could partially explain the coaction of both phytochromes in the cell.

**Keywords:** *Agrobacterium fabrum*; biliverdin; histidine kinase; phosphorylation; phytochrome; protein interaction

Phytochromes are photoreceptor proteins with a bilin chromophore that are found in plants, algae, fungi and bacteria [1]. As a common feature, phytochromes switch between the red-absorbing form Pr and the far-red-absorbing form Pfr by light. A typical phytochrome contains an N-terminal photosensory core module consisting of PAS [2], GAF [3] and phytochrome (PHY) domains and a C-terminal histidine kinase (HK) module [4,5]. In plants, multiple processes such as seed germination, seedling de-etiolation and flowering are under phytochrome control [6]. Fungal phytochromes control the differentiation between sexual and vegetative development and are involved in stress regulation [7]. In some photosynthetic bacteria, phytochromes control photosynthesis-related proteins and photosynthesis pigments [8,9], whereas in the non-photosynthetic soil bacterium *Agrobacterium fabrum*,

gene transfer to plants and conjugation are controlled by phytochrome [10,11]. Phytochromes are dimeric proteins which typically consist of two identical subunits. In organisms with several phytochromes, the formation of heterodimers is possible. Indeed, of the five different phytochromes phyA to phyE in the model plant *Arabidopsis thaliana*, phyB, phyC, phyD and phyE can form heterodimers [12]. Signal transmission in plants is mediated through phytochrome-interacting proteins such as the transcriptional regulators 'phytochrome-interacting factors' [13,14], the cytosolic proteins nucleotide diphosphate kinase 2 [15–17] and phytochrome kinase substrate 1 [18–20], phytochrome-associated protein phosphatase 5 [21] or other proteins [22–24]. Fungal phytochrome also acts through modulation of gene activity, and an interaction with velvet A and the blue light receptor system (LreA/LreB) have

## Abbreviations

BV, biliverdin; FRET, fluorescence resonance energy transfer; HK, histidine kinases; SEC, size exclusion chromatography.

been described [25]. Phytochrome signal transmission in bacteria such as *Bradyrhizobium* species and *Rhodospseudomonas palustris* involves gene activation by the phytochrome-interacting transcription factor PpsR [26,27]. Most bacterial phytochromes are light-regulated HK and it is generally assumed that the kinase has a signal transmitting function [28,29]. The first step of autophosphorylation at a conserved His residue is followed by a transphosphorylation from this His to a conserved Asp on a response regulator protein. Functions of response regulators of bacterial phytochromes are unknown and other interaction partners of bacterial phytochromes have so far not been identified. Knowing interaction partners and the modes of interaction will unveil the puzzle of signal transduction in a given organism.

Bacterial and fungal phytochromes use biliverdin (BV) as a chromophore [30]. In *A. fabrum*, there is one pair of phytochromes, Agp1 and Agp2 [31,32], where the chromophore is covalently bound to a Cys at the position 20 or 13 in Agp1 or Agp2 respectively (see Fig. 1 for protein domain structures and chromophore) [29,33,34]. Both phytochromes have different dark states, which are Pr in Agp1 and Pfr in Agp2 [33,35]. The HK of Agp1 belongs to the classical HKs, whereas Agp2 carries a HK of the HWE HK type which is defined by the presence of a conserved His together with a Trp-X-Glu motif and no recognizable 'F box' [30,36], a motif in the ATPase region of classical His kinases which is defined by a conserved Phe residue. The response regulator of Agp1 is a separate protein [28,29], whereas the response regulator of Agp2 comprises the C terminus of the phytochrome. Phytochromes with HKs and a C-terminal response regulator are also found in other bacteria and in fungi.

Spectral properties of phytochromes are determined by the interaction of the chromophore with amino acid residues of the chromophore pocket. A change of UV-vis spectra could be indicative of changes within this pocket, resulting from changes of the environment or from protein-protein interaction. Indeed, spectra of phytochromes are pH dependent [37,38]. For Agp1 and other phytochromes, it has been found that spectral properties are affected by temperature [39,40]. Evidence for the interaction of an unknown protein with Agp2 has been provided from spectral changes that occur upon mixing of Agp2 with the cell extract from an *Agrobacterium agp1<sup>-</sup>/agp2<sup>-</sup>* double knockout mutant [41]. Similarly, the autophosphorylation could be affected by environmental conditions and protein interactions.

The conjugation process of *A. fabrum* is initiated by a protein termed TraA. TraA proteins have three

functions, relaxase or cleavage of the DNA at the position of oriT, helicase and covalent binding to the single-stranded DNA. This protein-DNA adduct is transferred through pili to the recipient cell. There are three TraA homologues in *A. fabrum*, encoded by the linear chromosome, the At-plasmid and the Ti-plasmid [31,32,42]. Donor cells that carry a Ti-plasmid have a higher conjugation rate than strains without [41] indicating that the TraA protein encoded by the Ti-plasmid confers efficient conjugation. Donor cells in which the *agp1* or *agp2* gene is deleted have a lower conjugation rate than wild-type donor cells. In the double knockout mutant, conjugation is blocked. Thus, both phytochromes act together in the regulation of conjugation. We therefore suggested that both phytochromes might interact with each other and with TraA. Here, we analysed whether Agp1 and Agp2 would interact with each other *in vitro*.

## Materials and methods

### Expression vectors and Agp2 mutants

For Agp1 and Agp2, the expression vectors pAG1 [29] and pSA2 [43] were used respectively. Both expression vectors encode for full length proteins with C-terminal 6xHis affinity tags. The mutants Agp2\_D783A and Agp2\_D783N were made following the Quik Change protocol (Agilent, Santa Clara, CA, United States) using pSA2 as template. The primers for each mutant are given in Table 1.

### Protein expression and purification and holoprotein assembly

Agp1 and Agp2 were expressed and purified as apoproteins as described earlier in more detail [29,43,44]. Following IPTG-induced expression, extraction with a French pressure cell press, centrifugation and 50% ammonium sulphate precipitation, the proteins were purified by Ni-affinity chromatography. Pooled protein containing fractions were again subjected to 50% ammonium sulphate precipitation and dissolved in 50 mM Tris/Cl, 5 mM EDTA, 300 mM NaCl, pH 7.8. The ammonium sulphate concentration was ~ 50 mM as measured by electric conductivity. Typical protein concentrations at this stage of purification were 20 µM. BV (Sigma-Aldrich, Munich, Germany) was pre-purified by loading BV in aqueous solution to 1 mL Sep-Pak C18 cartridges (Waters, Milford, MA, United States), washing with water and elution in methanol. Purified BV was finally brought into DMSO at stock concentrations of 2–10 mM. To obtain holoprotein, apoprotein was incubated with BV at twofold molar excess for 2 h at room temperature. Holoprotein was passed through NAP 10 columns (GE healthcare, Munich, Germany) to remove free BV and

**Table 1.** Primer sequences for site-directed mutagenesis. F: forward primer; R: reverse primer.

Purpose	Gene	Primer sequence (5'-3')
Site-directed mutagenesis	<i>Agp2_D783A</i>	F: GGAACCAAGATTGATGGCGAGAATGGCGACGTC R: GACGTCGCCATTCTCGCCATCAATCTTGGTTCC
	<i>Agp2_D783N</i>	F: GGAACCAAGATTGATGTTGAGAATGGCGACGTCAG R: CTGACGTCGCCATTCTCAACATCAATCTTGGTTCC

ammonium sulphate. In cases where apoprotein was used for phosphorylation or assembly experiments, usually the same NAP separation was performed to remove residual ammonium sulphate. The buffer was 50 mM Tris/Cl, 5 mM EDTA, 300 mM NaCl, pH 7.8. The proteins were stored at  $-80^{\circ}\text{C}$ . Both Agp1 and Agp2 were essentially pure after purification. On SDS/PAGE, only a single band was observed (Fig. S1).

To follow the assembly of Agp1 or Agp2, apoprotein was mixed with BV directly in the photometer cuvette to yield final concentrations of  $1\ \mu\text{M}$  each, and UV/vis spectra were recorded directly after the mixing or the absorbance at a given wavelength was recorded over time in 1 s intervals. The same kind of measurements was also performed after addition of holo-Agp1 or holo-Agp2 to final concentrations of  $5\ \mu\text{M}$ . Protein concentrations were determined by measuring  $A_{280\ \text{nm}}$ , and the BV concentrations were obtained by measuring  $A_{696\ \text{nm}}$  in methanolic/HCl using an extinction coefficient of  $30.8\ \text{mM}^{-1}\cdot\text{cm}^{-1}$  [45].

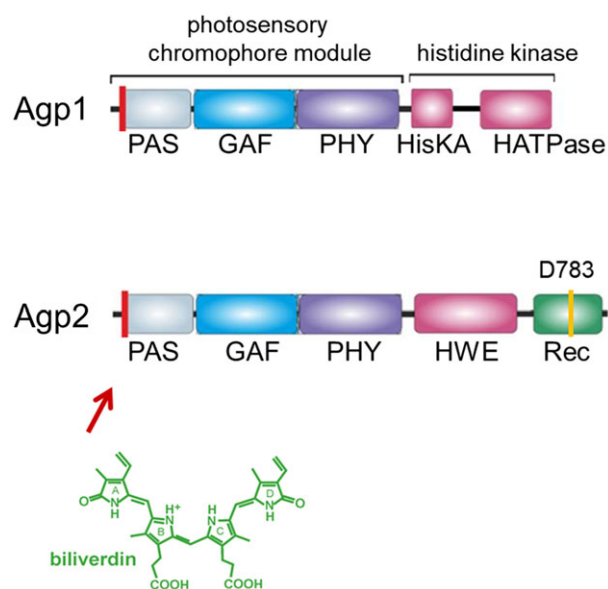


**Fig. 1.** Domain arrangements of Agp1 and Agp2. The photosensory chromophore module consists of the PAS, GAF and PHY domains. The positions of the BV-binding cysteines are indicated by the red lines. The position of the Asp residue in the response regulator of Agp2 that is homologous to the phosphoaccepting residues in typical response regulators is indicated by an orange line. This residue was mutated to Asn or Ala.

## Irradiation and photometry

If the Pr form of Agp1 was required, the protein was either kept in darkness after chromophore assembly or used after a  $> 2\ \text{h}$  dark incubation at  $25^{\circ}\text{C}$ . Dark reversion converts more than 90% Pfr back to Pr. For the Pfr form of Agp2 and the mutants thereof, the same procedure was followed. During 2 h dark incubation, Agp2 is almost completely in the Pfr form. To obtain Pfr of Agp1 or Pr of Agp2 (and mutants thereof), the samples were irradiated for 2 min with red light-emitting diodes ( $20\ \mu\text{mol}\cdot\text{m}^{-2}\cdot\text{s}^{-1}$ ,  $\lambda_{\text{max}} = 644\ \text{nm}$  or  $32\ \mu\text{mol}\cdot\text{m}^{-2}\cdot\text{s}^{-1}$ ,  $\lambda_{\text{max}} = 655\ \text{nm}$ ) or far-red light-emitting diodes ( $1500\ \mu\text{mol}\cdot\text{m}^{-2}\cdot\text{s}^{-1}$ ,  $\lambda_{\text{max}} = 780\ \text{nm}$ ) respectively [33]. UV/vis spectra (scan speed  $1000\ \text{nm}\cdot\text{min}^{-1}$ ) were recorded with a Jasco V550 photometer at  $18^{\circ}\text{C}$  [41]. Final concentrations and volumes of Agp1 or Agp2 were  $5\ \mu\text{M}$  and 1 mL respectively.

## Size-exclusion chromatography

For size-exclusion chromatography (SEC), a Superdex 200 10/300GL column (GE Healthcare) was used. The running buffer was 50 mM Tris-HCl, 5 mM EDTA and 150 mM NaCl, pH 7.8, the separation was performed at a flow rate of  $0.1\ \text{mL}\cdot\text{min}^{-1}$  and a temperature of  $4^{\circ}\text{C}$ . Thyroglobulin (669 KDa), apoferritin (443 KDa),  $\beta$ -amylase (200 KDa), alcohol dehydrogenase (150 KDa), BSA (66 KDa), carboanhydrase (29 KDa) and blue dextran (2000 kDa; Sigma) were used as marker proteins. For Agp1 and Agp2, typically  $200\ \mu\text{L}$  samples with a protein concentration of  $4\ \mu\text{M}$  were applied. Protein elution was monitored at 280 nm.

## Phosphorylation

Autophosphorylation of Agp1 and Agp2 was performed and analysed according to earlier experiments [29]. In darkness, phytochrome samples were mixed with phosphorylation buffer without ammonium sulphate (final concentration 25 mM Tris/HCl pH 7.8, 5 mM  $\text{MgCl}_2$ , 4 mM  $\beta$ -mercaptoethanol, 50 mM KCl, 5% ethylene glycol,  $\sim 2.5\ \mu\text{M}$  phytochromes, 50  $\mu\text{M}$  ATP containing 0.37 MBq [ $\gamma$ - $^{32}\text{P}$ ]ATP) or with ammonium sulphate (final concentration 50 mM  $(\text{NH}_4)_2\text{SO}_4$ ) and incubated for 20 min at room temperature in darkness. Free phosphate was determined by the malachite green phosphate assay kit [46] (Sigma). To 80  $\mu\text{L}$  test sample, 780  $\mu\text{L}$  water and

150  $\mu\text{L}$  'Working Reagent' were added. For colour development, the mixture was incubated for 30 min at room temperature. Finally, the absorbance at 620 nm was measured.

### Fluorophore labelling and fluorescence resonance energy transfer

For fluorescence resonance energy transfer (FRET), Agp1 and Agp2 were labelled with Atto 565 and Atto 565 fluorescent dyes respectively (Atto-Tec, Siegen, Germany). The selected Atto dyes have a maleimide reactive group which binds covalently to cysteine thiol groups. DMSO stock solutions containing 10 mM of Atto dye were prepared and stored in  $-80^\circ\text{C}$  until further use. Labelling and spectral measurements were performed in 50 mM Tris/Cl, 5 mM EDTA, 300 mM NaCl, pH 7.8 in darkness or under green safelight.

We used a mutant of Agp1, Agp1-M500-K517C and wild-type Agp2 for labelling. Agp1-M500-K517C has two cysteines, one at position 20, to which the chromophore is covalently bound, and one at position 517. This mutant is described in an earlier publication [47]. Agp2 has seven cysteines. For labelling, the apoprotein concentrations were adjusted to 10  $\mu\text{M}$ . Then, 10 mM tris (2-carboxyethyl) phosphine (TCEP) and 30  $\mu\text{M}$  BV from aqueous and DMSO stock solutions were added. After completion of chromophore assembly, the samples were subjected to ammonium sulphate (50% saturation) precipitation to remove excess BV and TCEP and dissolved in the equal volume of buffer. The Atto dyes were then added to the protein solution to a final concentration of 15  $\mu\text{M}$ . Following incubation over night at  $4^\circ$ , free Atto was removed by NAP-10 (GE healthcare) size exclusion column. The samples were characterized by UV/vis spectroscopy. About one molecule Atto dye was incorporated in each protein. We assume that Agp2 is preferentially labelled at the most exposed position; however, for the present experiment, the exact labelling position is not relevant.

Fluorescence measurements were performed using a Jasco FP 8300 fluorimeter. The excitation wavelength was always set to 470 nm and emission spectra of single labeled Agp1 or Agp2 samples or mixed labeled samples were measured between 480 and 700 nm. The final protein concentration was 1  $\mu\text{M}$ .

### Computer analysis

Calculations (subtraction and addition of spectra, mean values, standard error calculations, etc.) were performed with Excel (Microsoft, Redmond, WA, United States); tri-exponential decay analysis and data presentation were performed with Origin 2017, Microcal, Northampton, MA, United States.

## Results

### Size-exclusion chromatography

An interaction between Agp1 and Agp2 would result in changes of the SEC pattern. We therefore compared SEC profiles of a sample that contains Agp1 and Agp2 with those of Agp1 and Agp2 alone. All four possible combinations of Pr and Pfr were tested. Each profile was characterized by one peak of an apparent molecular mass of the dimer (260 kDa in Agp1, 280 kDa in Agp2) and of three oligomer peaks in the range of 443 kDa to void volume (Fig. 2). Oligomers were only found when the separation was performed at a low flow rate of  $0.1\text{ mL}\cdot\text{min}^{-1}$ , which was, however, required for clear separation. At  $0.5\text{ mL}\cdot\text{min}^{-1}$ , only dimer peaks were obtained, as in earlier experiments [48]. We regard oligomer formation as an *in vitro* effect on the column which could result from the reduction of NaCl from 300 to 150 mM in the gel. In subsequent discussions, we concentrate on the dimers of Agp1 and Agp2.

The dimer peak of Agp2 was always broader than that of Agp1 with retardation to higher elution times (Fig. 2). This Agp2 profile suggests that a fraction eluted as monomer. The SEC profiles of mixed Agp1 and Agp2 samples were compared with SEC profiles of Agp1 and Agp2 which were added mathematically. A strong interaction between Agp1 and Agp2 dimers would result in a shift of the dimer peak to earlier elution times. The dimer peaks were always found at indistinguishable positions. However, at elution times that would correspond to the Agp2 monomer, the absorbances in the profile of the mixture are lower than those calculated as the sum of both Agp1 and Agp2 profiles. This could be indicative of an interaction of Agp2 monomers with Agp1. Each separation was performed three times. We found these differences in all six runs in which Agp2 was in the Pr form (Fig. 2B,D and repetition measurements). In those runs where Agp2 was in the Pfr form, a weak difference was observed in four of six cases (Fig. 2A,C and repetition measurements). Although the SEC profiles show that there is no strong interaction between Agp1 and Agp2, a weak interaction between both could be possible, especially with Agp2 in the Pr form.

### Dark conversion and UV/vis spectra

We then tested whether the dark conversion of Agp1 and Agp2 could be affected by the presence of the other protein. In these experiments, buffer or Agp2 was mixed with red-irradiated Agp1 and the

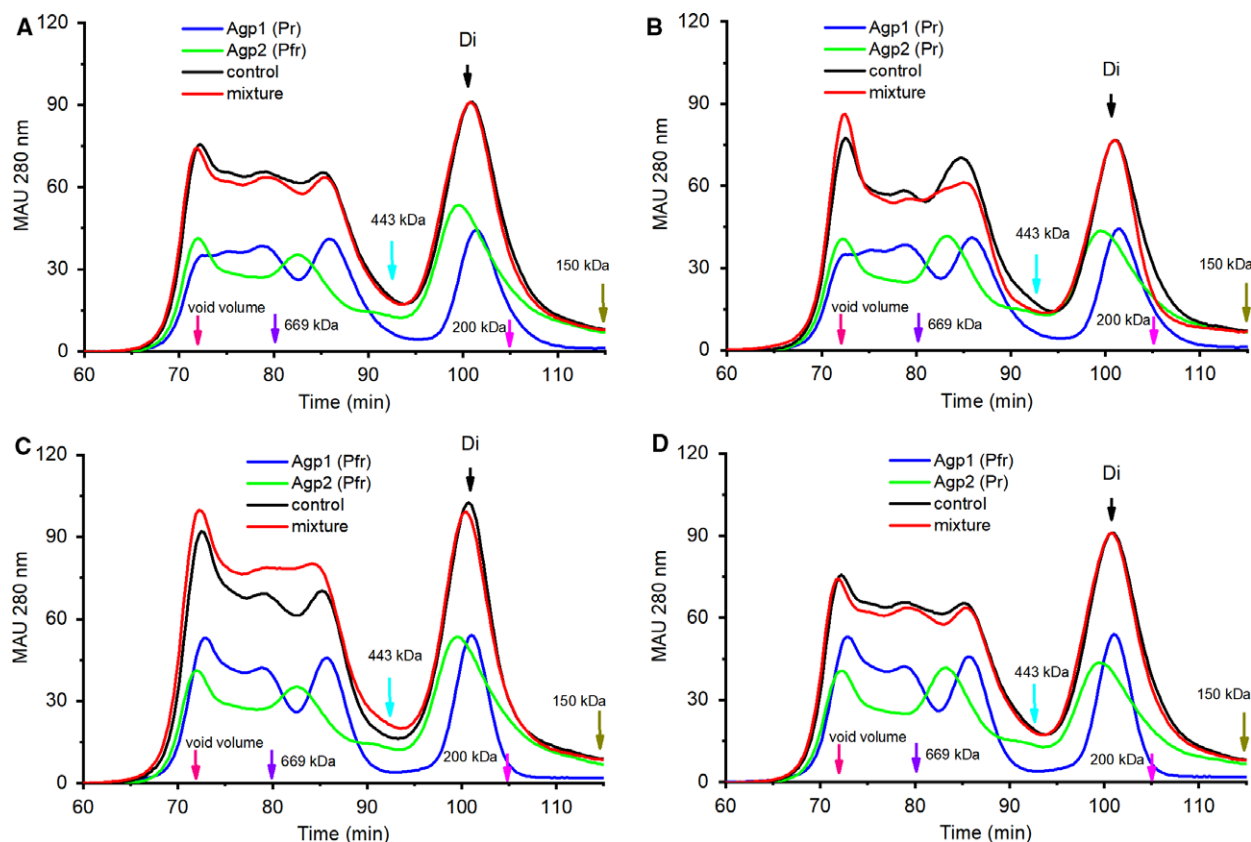


**Fig. 2.** SEC profiles of Agp1 (blue lines), Agp2 (green lines), mixed Agp1/Agp2 samples (mixture, red lines) and added profiles of Agp1 and Agp2 (control, black lines). Agp1 and Agp2 in Pr/Pfr forms (A), in Pr/Pr forms (B), in Pfr/Pfr forms (C) or in Pfr/Pr forms (D), respectively. For Pfr and Pr, the samples were irradiated with red or far-red light prior to mixing respectively. Either 200  $\mu$ L Agp1 (4  $\mu$ M) or Agp2 (4  $\mu$ M) alone or as a mixture (4  $\mu$ M Agp1, 4  $\mu$ M Agp2) was applied to the SEC column. The absorbance of the elution was recorded at 280 nm. The arrows indicate the elution times of marker proteins or the position of the Agp1 or Agp2 dimer peak ('Di').

absorbance time course was measured at 700 nm. The same procedures were performed with far-red-irradiated Agp2 mixed with buffer or with Agp1 and with time course measurements at 750 nm. All dark reversion kinetics could be fitted with triexponential decay functions (Fig. 3 and Table 2). The time constants  $t_1$ ,  $t_2$  and  $t_3$  of Agp2 measured in the presence of Agp1 were all smaller than those of the control which only contained Agp2. Similarly, the first and second dark reversion time constants of Agp1 with Agp2 were smaller than without Agp2, whereas the third time constants were similar with and without Agp2 (Table 2).

In order to test effects of possible protein interaction on UV/vis spectra, we compared difference spectra of Agp1 and Agp2 as obtained by red and far-red irradiation with an equivalent difference spectrum of an Agp1/Agp2 mixed sample. In one set of experiments, we subtracted spectra of dark-adapted samples from spectra after far-red irradiation. This light treatment

affects mainly Agp2 but also Agp1 although to a smaller extent. The shape of the difference spectrum of the mixed sample was clearly different from the shape of the control difference spectrum, that is, the mathematically added Agp1 and Agp2 difference spectra. The mixed sample is characterized by a slightly positive absorbance difference in the 700 nm range, where the control difference spectrum is only negative (Fig. 4C). As a consequence, the double difference spectrum shows a maximum at  $\sim$  700 nm and resembles a Pr spectrum in the range from 600 to 800 nm.

Another set of experiments was performed with red light instead of far-red light. Red light results mainly in Agp1 Pr to Pfr conversion and Agp2 converts only to a minor extent from Pfr to Pr. Also, in this experiment, the difference spectrum of the Agp1/Agp2 mixed sample differed from the added difference spectra of Agp1 and Agp2 (Fig. 4D). The double difference spectrum shows a maximum at  $\sim$  700 nm with a shoulder at  $\sim$  750 nm, features common to a typical Pfr

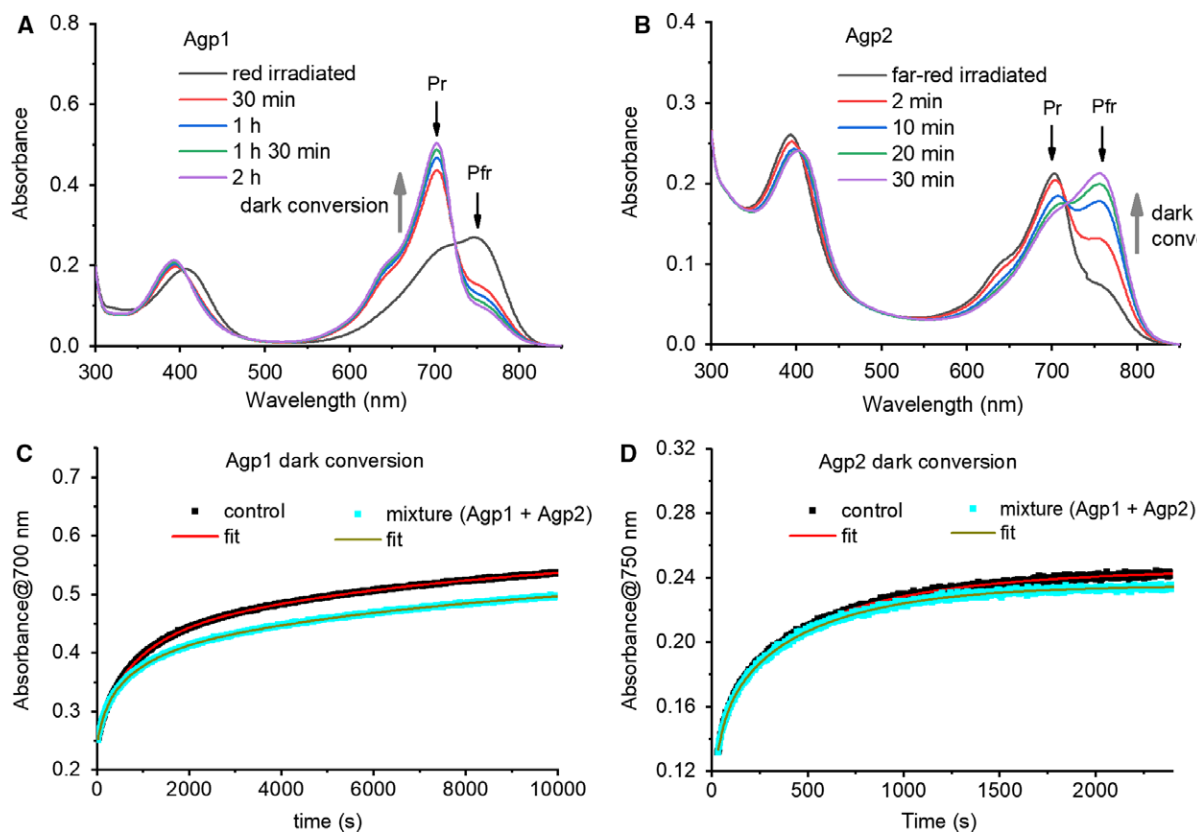


**Fig. 3.** Dark conversion of Agp1 after saturating red irradiation (A), with and without Agp2, measured at 700 nm (increase of Pr) (C). Dark reversion of Agp2 after saturating far-red irradiation (B), with and without Agp1, at 750 nm (increase of Pfr) (D). Each irradiation was performed prior to mixing. Experiments were repeated three times. Time constants and amplitudes of a three exponential fit are given in Table 1.

**Table 2.** Exponential fit for Agp1 and Agp2 dark conversion. A1, A2, A3: amplitudes; t1, t2, t3: time constants. The errors are from the fit. This is one example of three repetitions with similar results.

$$\text{Equation: } y = -A1 \cdot \exp(-x/t1) - A2 \cdot \exp(-x/t2) - A3 \cdot \exp(-x/t3) + y0$$

	Agp1		Agp2	
	In buffer	In Agp2	In buffer	In Agp1
A1	0.042 ± 0.002	0.051 ± 0.002	0.046 ± 0.002	0.034 ± 0.003
A2	0.13 ± 0.002	0.094 ± 0.001	0.041 ± 0.004	0.029 ± 0.003
A3	0.16 ± 0.0004	0.15 ± 0.0005	0.057 ± 0.005	0.069 ± 0.002
t1 (s)	208 ± 9	160 ± 6	45 ± 3	34 ± 6
t2 (s)	870 ± 20	790 ± 20	250 ± 30	130 ± 20
t3 (s)	7500 ± 200	7700 ± 200	790 ± 50	540 ± 10
R <sup>2</sup>	0.99985	0.9997	0.99854	0.99799

spectrum in the range from 600 to 800 nm. Both dark reversion and spectral measurements indicate protein interactions between Agp1 and Agp2.

### Histidine kinase autophosphorylation

Agp1 and Agp2 carry a HK region, and Agp2 has an additional response regulator at its C terminus [29,33].

We intended to study the effect of Agp1 and Agp2 on the phosphorylation activity of the respective other partner. Our group has performed several phosphorylation studies with Agp1 [29,39], but in phosphorylation trials with Agp2, we observed no or only a weak phosphorylation signal. A weak autophosphorylation band was always obtained when the sample contained residual ammonium sulphate from previous

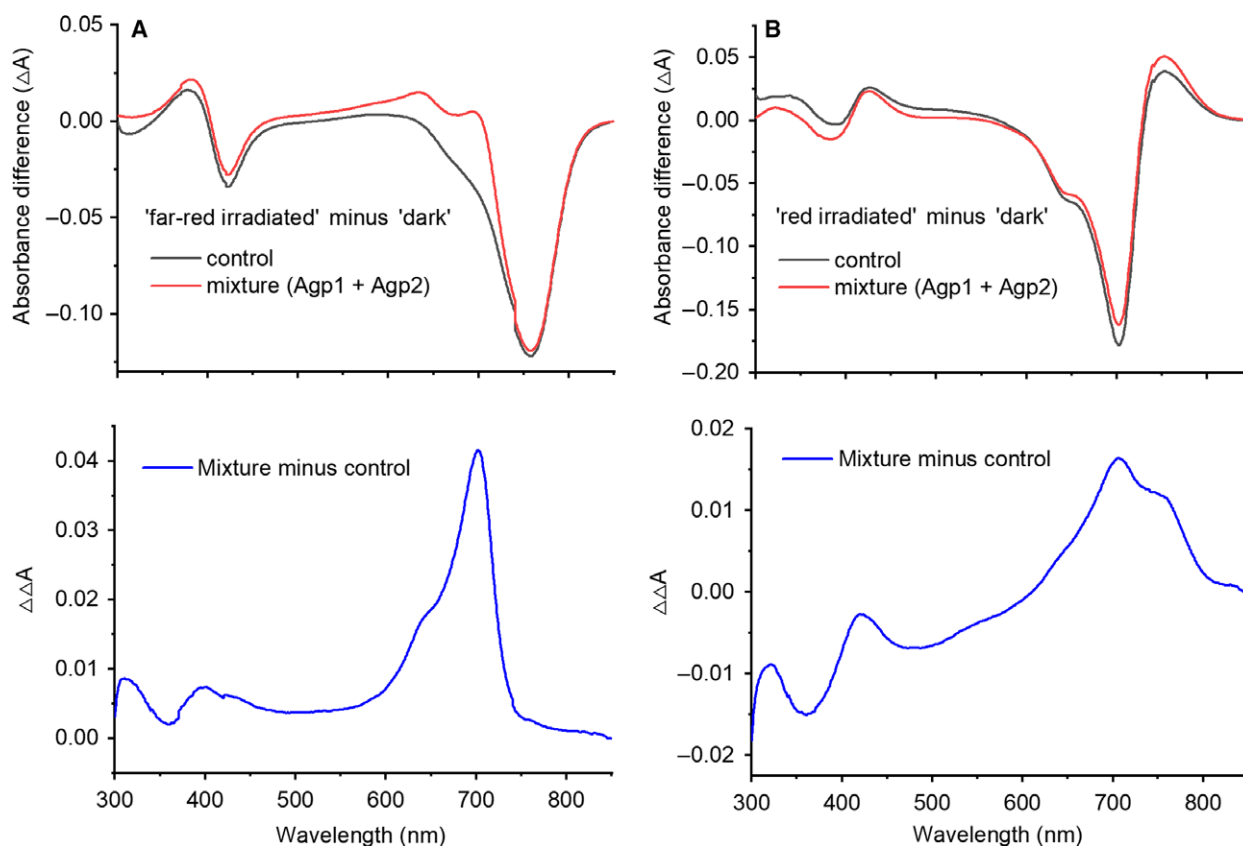


**Fig. 4.** Absorbance difference spectra of 'far-red (A)' or 'red (B) irradiated' minus 'dark' (above) and the double difference spectra of 'mixture' minus 'control' (Agp1 and Agp2 added; below). Control and mixture are depicted by black and red lines respectively. The spectra are representatives of three replicates.

precipitations (see Materials and methods), whereas no phosphorylation band was detected when ammonium sulphate-free Agp2 was used (Fig. 5A). Our initial interpretation of this observation was that the response regulator catalyses a rapid transphosphorylation and dephosphorylation [49] and that ammonium sulphate would inhibit this turnover. We therefore mutagenized the Asp783 residue of the Agp2 response regulator and tested the mutants for phosphorylation. According to the homology with other response regulators, one would expect Asp783 to accept the phosphate from the His residue in the His kinase [33]. The autophosphorylation signal of the Agp2\_D783A mutant was clearly visible and thus higher than wild-type Agp2, and the signal of Agp2\_D783N was even higher, that is, in the same range as Agp1 (Fig. 5B). A turnover of ATP that, as a net result, only yields weak or no protein phosphorylation would result in detectable free phosphate. We used an assay based on malachite green to detect free phosphate. After incubating Agp1, Agp2, Agp2\_D783A or Agp2\_D783N with ATP, no

free phosphate was detected (Fig. 6). Therefore, we rejected the hypothesis of response regulator-mediated dephosphorylation. When wild-type and the mutants of Agp2 were compared by SEC, clear mobility differences of the (proposed) dimers were observed. The apparent molecular mass was 280 kDa for Agp2, 292 kDa for Agp2\_D783A and 318 kDa for Agp2\_D783N (Fig. 7). These major differences show that the shape of the Agp2 protein is significantly affected by these mutations. The amino acids change from negatively charged Asp which can undergo ionic interactions in the wild-type protein to neutral Ala and Asn. The Asn mutant had the strongest phosphorylation signal and the biggest effect on SEC. This correlates with the fact that, of the three amino acid residues, Asn is the only one that can act as donor and acceptor of hydrogen bonds. We assume that, in wild-type Agp2, the response regulator module shields the histidine of the HWE domain so that autophosphorylation is inhibited and that the mutations result in partially or totally detached response regulator due

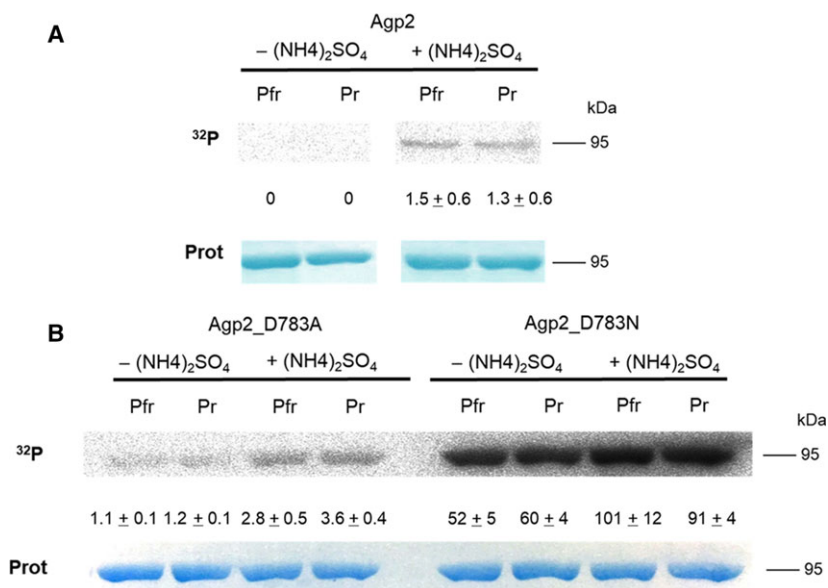


**Fig. 5.** Autophosphorylation of Agp2 (A) wild-type and (B) D783A and D783N mutants in the absence or presence of (NH<sub>4</sub>)<sub>2</sub>SO<sub>4</sub> (50 mM) as indicated above the panels. (A, B) The above panels show typical autoradiograms, the numbers printed under each autoradiogram give mean staining intensities ± SE of five replicates (staining intensity is the total pixel intensity in a rectangle area around the stained band after background subtraction). The incubation times of Agp2 with ATP-<sup>32</sup>P and film exposure times were always 20 min and 20 h respectively. This allows comparison of all signals between different blots. Coomassie stains of the same bands are shown in the panels below.

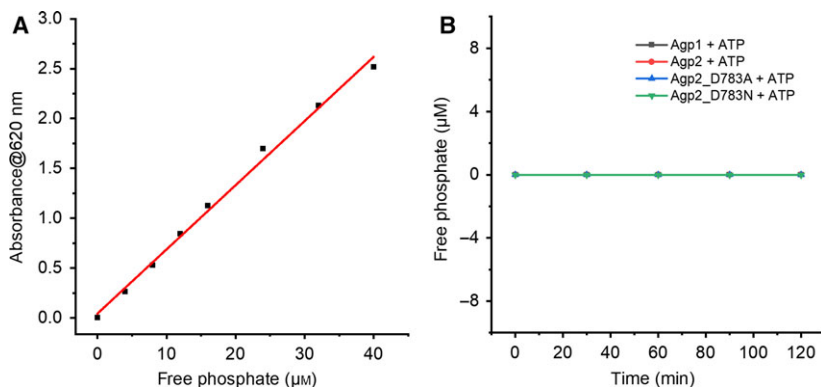


**Fig. 6.** Determination of free phosphate by the malachite green phosphate assay. Standard curve of phosphate (A) and phosphate concentrations after incubating Agp1, Agp2, Agp2\_D783A or Agp2\_D783N with ATP for different time in the dark (B). The assay was performed three times.

to the loss of ionic interactions. In Agp2\_D783N, the side chain of Asn783 may stabilize a conformation that is significantly different from Agp2\_D783A.

For phosphorylation of mixed Agp1/Agp2 samples, all four combinations of Pr and Pfr were analysed and compared with Agp1 and Agp2 alone in their Pr or Pfr forms. As a reference, the added phosphorylation signals of Agp1-Pr and Agp1-Pfr (each alone) set equal to 100. Because phosphorylation of wild-type Agp2 is not visible (ammonium sulphate was removed completely), these assays show only the impact of Agp2 on the phosphorylation of Agp1 but not vice versa. If Agp2 in either the Pfr or the Pr form was incubated with Agp1 in its Pr form, the relative phosphorylation signal of Agp1 was 52 ± 3 or 55 ± 2 respectively. The signal of Agp1 (in its Pr form) without Agp2 was significantly higher, that is, 72 ± 1. The Agp1 signal in the Pfr form was reduced as compared to Pr, in agreement with previous studies [29]. There was no clear

effect of Agp2 on phosphorylation of Agp1 in the Pfr form, no matter whether Agp2 was in the Pr or in the Pfr form (Fig. 8A).

In order to test the impact of Agp1 on the phosphorylation of Agp2, we performed the same mixing experiments with Agp1 and Agp2\_D783N, which revealed strong phosphorylation activity. There was again an impact of Agp2\_D783N on the phosphorylation of Agp1 in the Pr form, irrespective of whether the Agp2 mutant was in the Pr or in the Pfr form. In addition, and unlike for wild-type Agp2, also the Pfr signal of Agp1 was diminished by Agp2\_D783N. The relative phosphorylation signals of Agp2\_D783N in the Pfr and Pr forms were 38 ± 1 and 39 ± 3 respectively. The Pfr signal decreased to 32 ± 2 and 30 ± 3 in the presence of Agp1 in its Pr and Pfr forms respectively. The signal of the Pr form of Agp2\_D783N was reduced to 31 ± 1 by Agp1 in its Pfr form. Agp1 in its Pfr form caused a slight increase in the Agp2\_D783N

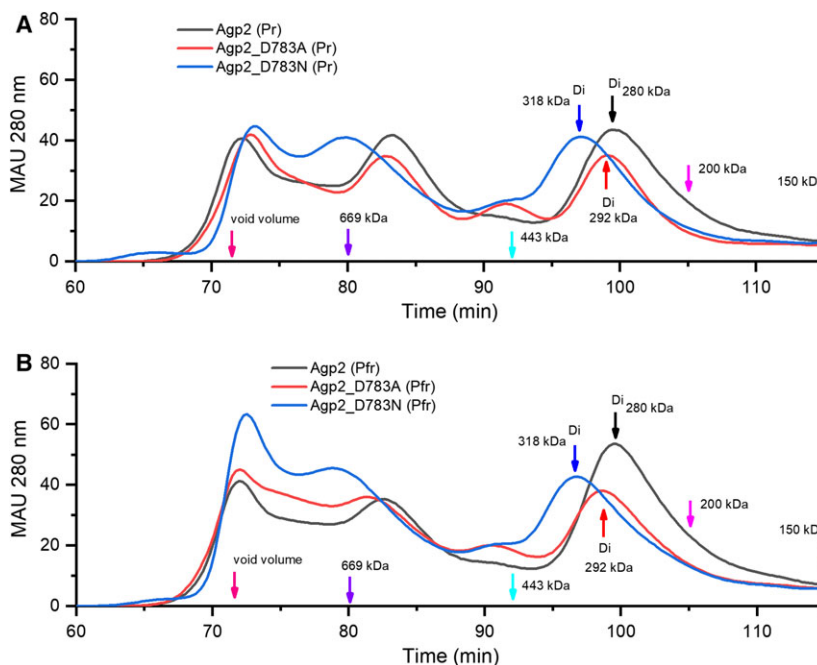


**Fig. 7.** SEC analysis of Agp2 (black lines), Agp2\_D783A (red lines) and Agp2\_D783N (blue lines) in Pr (A) and Pfr forms (B). The protein concentrations were 4  $\mu$ M. The SEC elution profiles were recorded at 280 nm. Arrows indicate the positions of the marker proteins or the positions of the Agp1 or Agp2 dimer ('Di').

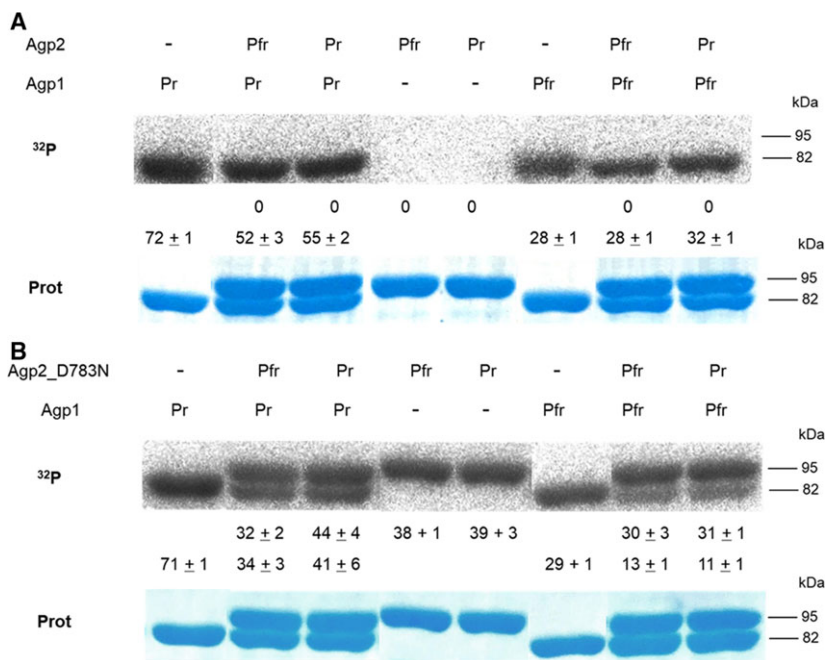


**Fig. 8.** Autophosphorylation of Agp1 and Agp2/Agp2\_D783N. The upper panels show typical autoradiogram images, the lower panels show Coomassie stained bands of the same gel. The bands are from the same gel but rearranged in sequence. For Pr of Agp1 and Pfr of Agp2, the dark incubated samples were used directly. For Pfr of Agp1 and Pr of Agp2, the samples were irradiated with red or far-red light prior to mixing respectively. ATP- $\gamma$ - $^{32}$ P incubation and film exposure times were always 20 min and 2 h respectively. The bands at 95 and 82 kDa refer to Agp2 and Agp1 respectively. The numbers underneath the autoradiograms stand for mean values of 5 relative staining intensities  $\pm$  SE. For relative staining intensity, the sum of pixel intensities of Agp1-Pr and Agp1-Pfr was set as 100. (A) Agp1 and Agp2 wild-type were incubated alone or together with ATP- $\gamma$ - $^{32}$ P. There is no Agp2 phosphorylation signal, because the samples were devoid of ammonium sulphate. (B) Agp1 and the D783N mutant of Agp2 were incubated alone or together with ATP- $\gamma$ - $^{32}$ P.

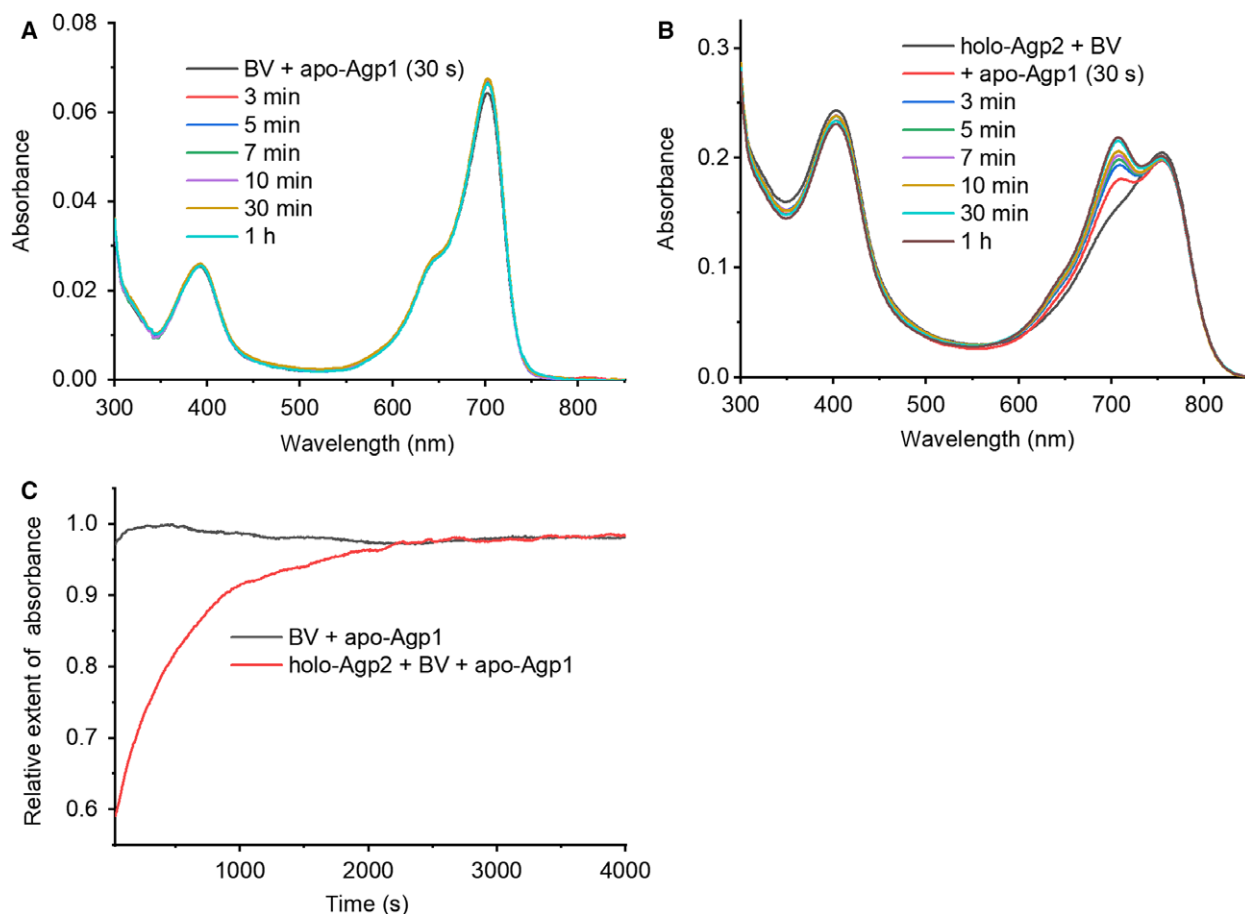


**Fig. 9.** (A) UV/vis spectra recorded during assembly of Agg1 with BV. (B) UV/vis spectra recorded during assembly of Agg1 with BV in the presence of holo-Agg2. (C) Time drive measurements of the 700 nm absorbance during Agg1 assembly, black line: apo Agg1 and BV, red line: holo-Agg2, apo-Agg1 and BV (the absorbance of holo-Agg2 was set as 0). Both lines were scaled to a final value of 1. BV binding to apo-Agg1 without (A) or with (B) holo-Agg2 monitored by absorption spectra at different incubation times, and relative extents of absorbance at 700 nm for the two mixtures (C).

signal to  $44 \pm 4$ . Thus, phosphorylation of both phytochromes can be slightly affected by the presence of the other phytochrome. The effect of Agg2 in its Pr or Pfr form on Agg1-Pr was the strongest (Fig. 8B). Since the concentration of phytochromes was  $\sim 2.5 \mu\text{M}$  and that of ATP  $50 \mu\text{M}$ , we exclude a competition effect between Agg1 and Agg2.

### Chromophore assembly

We also tested the impact of Agg1 and Agg2 on the BV assembly of the other protein. In the control measurements, BV was mixed with the apoproteins apo-Agg1 or apo-Agg2 and the absorbance kinetics were followed at 700 or 750 nm respectively. In the mixed samples, either the apo-Agg2/BV sample was added to Agg1 holoprotein or the apo-Agg1/BV sample added to Agg2 holoprotein. We found that the assembly of

either phytochrome was strongly affected by the presence of the respective other phytochrome (in its holo form). Although the absorbance changes of Agg1 were apparently complete after  $\sim 2$  min, as in earlier studies [29], it took about 40 min for the completion in the presence of Agg2 (Fig. 9). On the contrary, holo-Agg1 shortened the time of spectral changes during Agg2 assembly from 1 h (see also [33]) to 25 min (Fig. 10). These drastic effects could result from protein interactions between Agg1 and Agg2. Agg2 could alter the protein conformation of Agg1 apoprotein so that chromophore accession for Agg1 is hindered.

### FRET of Agg1 and Agg2

Fluorescence resonance energy transfer is another method for studying protein interaction. We labelled Agg1-M500-K517C, a mutant of Agg1, with Atto 565

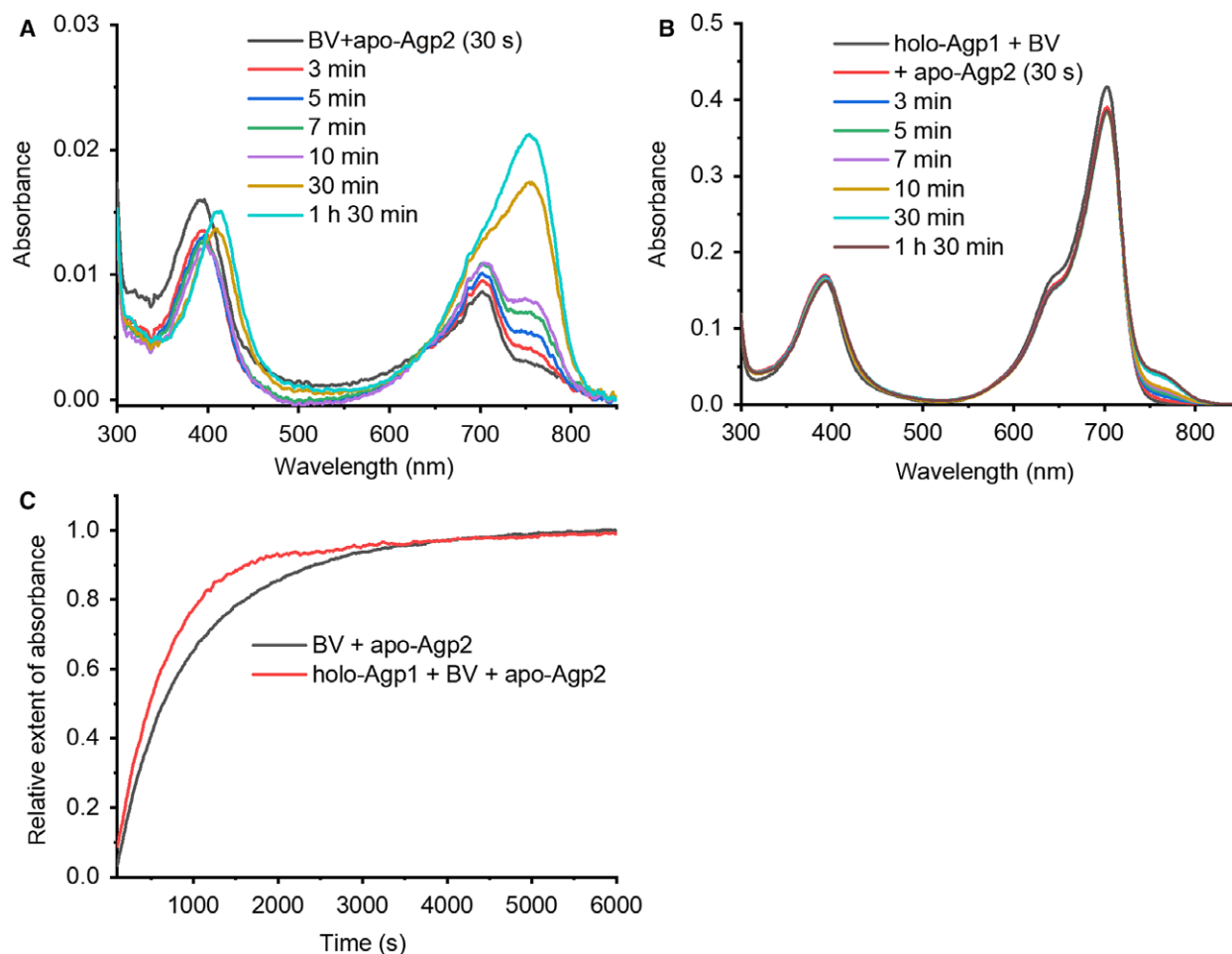


**Fig. 10.** (A) UV/vis spectra recorded during assembly of Agp2 with BV. (B) UV/vis spectra recorded during assembly of Agp2 with BV in the presence of holo-Agp1. (C) Time drive measurements of the 750 nm absorbance during Agp2 assembly, black line: apo Agp2 and BV, red line: holo-Agp1, apo-Agp2 and BV (the absorbance of holo-Agp1 was set as 0). Both lines were scaled to a final value of 1. BV binding to apo-Agp1 without (A) or with (B) holo-Agp2 monitored by absorption spectra at different incubation times, and relative extents of absorbance at 700 nm for the two mixtures

(acceptor) and Agp2 with Atto 495 (donor, for details, see Materials and methods section). The measurements are shown in Fig. 11. When single labelled proteins were excited at 470 nm, characteristic emission spectra with peaks at 525 and 590 nm were obtained, confirming the efficient labelling. The emission of labelled Agp1-M500-K517C is weaker than that of labelled Agp2, because the exiting light is much less absorbed by Atto 565 than by Atto 485. The Agp1-M500-K517C/Agp2 mixed sample is characterized by a two peak emission, as expected. The fluorescence intensity in the 530 nm range was lower than that of the corresponding Agp2 sample without Agp1-M500-K517C. The emission at 590 nm was higher than the calculated added emission of both single labelled proteins (see also legend of Fig. 11). Both the reduction of fluorescence emission of

the donor and gain of fluorescence of the acceptor are features of characteristic FRET and indicative for an interaction of Agp1-M500-K517C and Agp2. To study the interaction possibility between Agp1 and Agp2, FRET experiments were also analysed and fluorescence spectra of Agp1, Agp2 and their mixture were measured and compared. For this purpose, Agp2 wild-type and a mutant of Agp1 were used.

## Discussion

Conjugation of *A. fabrum* is controlled by light, mediated through phytochrome Agp1 and Agp2. The protein TraA has a central role in the conjugation process. This relaxase cleaves a single strand in the plasmid DNA, binds covalently to the DNA end and separates both

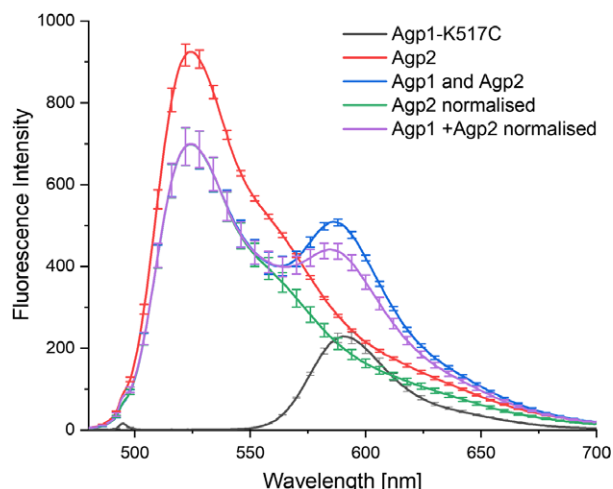


**Fig. 11.** Emission spectra of Atto 565-labelled Agp1-M500-K517C (black line), Atto 495-labelled Agp2 (red line) and a mixture of both samples (blue line). The spectrum of labelled Agp2 was normalized so that its peak value is identical to that of the mixed sample (green line). The normalized spectrum and the emission spectrum of labelled Agp2 were added (violet line). The peak emission of the mixed sample (blue line) was above that of this calculated spectrum. The excitation wavelength was 470 nm. The curves indicate mean values of four independent experiments; the error bars represent the standard error.

strands [50,51]. TraA could be regulated by the phytochromes through indirect mechanisms or through a direct interaction between the proteins. Since both Agp1 and Agp2 contribute to a similar extent to conjugation [11], we tested here for an interaction between both proteins *in vitro*. We performed one standard assay for protein–protein interaction, SEC. In SEC, proteins undergo rapid dilution upon entering the gel matrix. Therefore, a change in elution maxima is obtained only for tightly interacting proteins. Nevertheless, subtle changes of elution profiles were found for mixed Agp1/Agp2 samples, an indication for weak interactions between both phytochromes. The theory of weak interaction between Agp1 and Agp2 is supported by UV-vis absorbance spectra, dark reversion, phosphorylation, chromophore assembly experiments. In these assays, the properties of one protein were slightly changed by the presence of the other protein. Furthermore, FRET studies on labelled Agp1 and Agp2 confirmed the interaction hypothesis.

In our studies, Agp2 revealed no autophosphorylation signal. This result conflicts with earlier reports of Karniol *et al.* [33] who published a strong and Pr/Pfr-dependent signal for Agp2. The fungal phytochrome FphA, another phytochrome with a C-terminal response regulator, also showed a clear autophosphorylation signal, but there was no difference between Pr and Pfr [52]. In our Agp2 phosphorylation studies, weak and strong

autophosphorylation was obtained for the Agp2\_D783A and Agp2\_D783N mutants, respectively, in which the putative receiver amino acid of the response regulator is mutated. We initially suggested that the missing phosphorylation signal of Agp2 could result from a rapid dephosphorylation by the response regulator. Dephosphorylation activity is described for diverse response regulators [49]. Since no free phosphate was detected in our samples, however, we rejected the idea of rapid phosphate turnover. SEC pointed to a significant protein conformational change towards larger apparent molecular size induced by the mutations. This conformational shift is most likely dependent to a large extent on the presence or absence of a charge at position 783 of Agp2. The extent of SEC mobility changes of Agp2\_D783A and Agp2\_D783N correlates with the increased phosphorylation of these mutants. Therefore, the conformational change is probably the cause for the increase in phosphorylation. In the wild-type, the response regulator domain could cover the conserved histidine of the HWE HK and block autophosphorylation. This conformation could be stabilized by ionic interactions involving Asp783. Loss of the negative charge at this position as induced by mutagenesis could result in a more open conformation, thus allowing autophosphorylation. The D783A and D783N mutants were generated in order to find out whether Agp1 has an impact on the autophosphorylation of Agp2 and it was possible to demonstrate such an effect. As side effect, the mutants also provided an indirect insight into the Agp2 phosphorylation mechanism. We observed no phosphorylation difference between Pr and Pfr of Agp2\_D783N, and no evidence for a phosphotransfer from the HWE His kinase to the response regulator but instead major conformational changes of the protein as induced by the charge or its loss at one position of the response regulator. For these reasons, we propose that Agp2 does not signal through the His kinase → response regulator pathway. *In vivo*, Agp2 autophosphorylation could be dependent on the impact of other molecules and this could result in a modulation of signalling activity. Combined structural studies [53] and molecular/physiological work must be continued to unravel details of signal transduction.

A strong effect that appears to be induced by Agp1/Agp2 interaction was found in chromophore assembly studies; the kinetics of both Agp1 and Agp2 were affected by the respective other phytochrome. In order to avoid competition effects, we used holoproteins to test for an effect on the assembly of the apoprotein partner. Phytochrome chromophore assembly has been investigated several times by time-resolved spectroscopy [54], but structural details

behind this process are unclear. The chromophore pocket of the holoprotein appears as a close container which has no access from outside [55]. The structure of the apoprotein is unknown, but the chromophore pocket must be different from the holoprotein and adopt a more open conformation to provide access for the chromophore from outside. Assembly kinetics vary significantly between Agp1, Agp2 and other phytochromes [55–57]. These differences could be based on different openings of the chromophore pockets of the apoproteins. The drastic slowdown of Agp1 assembly observed here upon Agp2 addition might result from a closure of the open chromophore pocket of Agp1. The weak interaction between Agp1 and Agp2 as predicted above suggests that Agp1 and Agp2 switch rapidly between the bound and the non-bound state and that the non-bound state is the preferred state. The strong effect of protein–protein interaction on the chromophore assembly, however, requires additional assumptions. If, for example, Agp1 and Agp2 associate for half the time with each other and if the chromophore pocket of Agp1 is closed in the bound state, but open in the non-bound state, chromophore assembly would be half as fast as for Agp1 alone. We must therefore assume that Agp1 chromophore assembly is affected in the Agp1/Agp2 bound and in the non-bound state and that the chromophore pocket remains closed for a certain time upon dissociation of both proteins. In a similar way, the impact of Agp1 on the assembly of Agp2 may be discussed, although the effect goes to the opposite direction: the Agp2 assembly is accelerated by the addition of Agp1. Agp1 could open the chromophore pocket of Agp2 for a more rapid chromophore incorporation. Here, three different states may be required: open chromophore pocket (Agp2 apoprotein during interaction with Agp1), partially open chromophore pocket (Agp2 apoprotein) and closed chromophore pocket (Agp2 holoprotein, as seen in the crystal structure [53]). It is interesting to see that the slow assembly of Agp2 is accelerated by Agp1 and the fast assembly of Agp1 decelerated by Agp2. Fluorescence measurements on Atto labelled Agp1 and Agp2 showed that energy is transferred from the Agp2 donor to the Agp1 acceptor, which is only possible if the fluorophores are at a distance of < 10 nm. The now established method allows, for example, to study fragments of Agp1 and Agp2, testing for differences between Pr/Pfr and also the interaction between recombinant TraA and Agp1 or Agp2 in the future.

Taken together, we have found evidence for a weak interaction of Agp1 and Agp2 by different methods. This is, to our knowledge, the first study of this kind for bacterial phytochromes. The heterodimers formed

between different types of plant phytochromes are another example for interactions between different phytochromes. However, recombinant Agp1 forms tight homodimers that do probably not dissociate [48] and we believe it unlikely that Agp1/Agp2 heterodimers are formed in solution. We could imagine either interactions between Agp2 monomers and Agp1 dimers or – more likely – complexes formed between Agp1 dimers and Agp2 dimers. An interaction with another protein *in vivo*, like TraA, could further stabilize the interaction between Agp1 and Agp2.

## Acknowledgements

We thank Nadja Wunsch for technical help. This work was supported by the China Scholarship Council (to PX) and a DFG grant LA799/18-1 to NK and TL.

## Author contributions

TL and NK designed the research; PX performed experiments; AE contributed to fluorescence measurements; AK contributed to protein phosphorylation; HM and AE contributed to protein purification; AA and RF contributed to size-exclusion chromatography; PX, GK and TL analysed the data and wrote the manuscript with input from NK.

## References

- 1 Beattie GA, Hatfield BM, Dong HL and McGrane RS (2018) Seeing the light: the roles of red- and blue-light sensing in plant microbes. In *Annual Review of Phytopathology*, Vol 56 (Leach JE and Lindow SE, eds), pp. 41–66. Annual Reviews, Palo Alto, CA.
- 2 Aravind L and Ponting CP (1999) The cytoplasmic helical linker domain of receptor histidine kinase and methyl-accepting proteins is common to many prokaryotic signalling proteins. *FEMS Microbiol Lett* **176**, 111–116.
- 3 Aravind L and Ponting CP (1997) The GAF domain: an evolutionary link between diverse phototransducing proteins. *Trends Biochem Sci* **22**, 458–459.
- 4 Rockwell NC, Su YS and Lagarias JC (2006) Phytochrome structure and signaling mechanisms. *Annu Rev Plant Biol* **57**, 837–858.
- 5 Buchberger T and Lamparter T (2015) Streptophyte phytochromes exhibit an N-terminus of cyanobacterial origin and a C-terminus of proteobacterial origin. *BMC Res Notes* **8**, 144.
- 6 Kendrick RE and Kronenberg GHM (1994) *Photomorphogenesis in Plants*, 2nd edition, 2nd edn. Kluwer Academic Publishers, Dordrecht.

- 7 Yu ZZ, Armant O and Fischer R (2016) Fungi use the SakA (HogA) pathway for phytochrome-dependent light signalling. *Nat Microbiol* **1**, article number 16019. <https://doi.org/10.1038/Nmicrobiol.2016.19>.
- 8 Giraud E, Fardoux J, Fourrier N, Hannibal L, Genty B, Bouyer P, Dreyfus B and Vermeglio A (2002) Bacteriophytochrome controls photosystem synthesis in anoxygenic bacteria. *Nature* **417**, 202–205.
- 9 Giraud E, Zappa S, Jaubert M, Hannibal L, Fardoux J, Adriano JM, Bouyer P, Genty B, Pignol D and Vermeglio A (2004) Bacteriophytochrome and regulation of the synthesis of the photosynthetic apparatus in *Rhodospseudomonas palustris*: pitfalls of using laboratory strains. *Photochem Photobiol Sci* **3**, 587–591.
- 10 Oberpichler I, Rosen R, Rasouly A, Vugman M, Ron EZ and Lamparter T (2008) Light affects motility and infectivity of *Agrobacterium tumefaciens*. *Environ Microbiol* **10**, 2020–2029.
- 11 Bai Y, Rottwinkel G, Feng J, Liu Y and Lamparter T (2016) Bacteriophytochromes control conjugation in *Agrobacterium fabrum*. *J Photochem Photobiol, B* **161**, 192–199.
- 12 Sharrock RA and Clack T (2004) Heterodimerization of type II phytochromes in Arabidopsis. *Proc Natl Acad Sci USA* **101**, 11500–11505.
- 13 Ni M, Tepperman JM and Quail PH (1998) PIF3, a phytochrome-interacting factor necessary for normal photoinduced signal transduction, is a novel basic helix-loop-helix protein. *Cell* **95**, 657–667.
- 14 Kami C, Hersch M, Trevisan M, Genoud T, Hiltbrunner A, Bergmann S and Fankhauser C (2012) Nuclear phytochrome a signaling promotes phototropism in Arabidopsis. *Plant Cell* **24**, 566–576.
- 15 Tanaka N, Ogura T, Noguchi T, Hirano H, Yabe N and Hasunuma K (1998) Phytochrome-mediated light signals are transduced to nucleoside diphosphate. *J Photochem Photobiol, B*, **45**, 113–121.
- 16 Choi G, Yi H, Lee J, Kwon YK, Soh MS, Shin B, Luka Z and Song PS (1999) Phytochrome signalling is mediated through nucleoside diphosphate kinase 2. *Nature* **401**, 610–613.
- 17 Shen Y, Kim JI and Song PS (2005) NDPK2 as a signal transducer in the phytochrome-mediated light signaling. *J Biol Chem* **280**, 5740–5749.
- 18 Fankhauser C, Yeh KC, Lagarias JC, Zhang H, Elich TD and Chory J (1999) PKS1, a substrate phosphorylated by phytochrome that modulates light signaling in Arabidopsis. *Science* **284**, 1539–1541.
- 19 Lariguet P, Schepens I, Hodgson D, Pedmale UV, Trevisan M, Kami C, De Carbonnel M, Alonso JM, Ecker JR, Liscum E *et al.* (2006) Phytochrome kinase substrate 1 is a phototropin 1 binding protein required for phototropism. *Proc Natl Acad Sci USA* **103**, 10134–10139.
- 20 Schepens I, Boccalandro HE, Kami C, Casal JJ and Fankhauser C (2008) Phytochrome kinase substrate 4 modulates phytochrome-mediated control of hypocotyl growth orientation. *Plant Physiol* **147**, 661–671.
- 21 Ryu JS, Kim JI, Kunkel T, Kim BC, Cho DS, Hong SH, Kim SH, Fernandez AP, Kim Y, Alonso JM *et al.* (2005) Phytochrome-specific type 5 phosphatase controls light signal flux by enhancing phytochrome stability and affinity for a signal transducer. *Cell* **120**, 395–406.
- 22 Kircher S, Kozma-Bognar L, Kim L, Adam E, Harter K, Schäfer E and Nagy F (1999) Light quality-dependent nuclear import of the plant photoreceptors phytochrome A and B. *Plant Cell* **11**, 1445–1456.
- 23 Al Sady B, Ni W, Kircher S, Schäfer E and Quail PH (2006) Photoactivated phytochrome induces rapid PIF3 phosphorylation prior to proteasome-mediated degradation. *Mol Cell* **23**, 439–446.
- 24 Castillon A, Shen H and Huq E (2007) Phytochrome interacting factors: central players in phytochrome-mediated light signaling networks. *Trends Plant Sci* **12**, 514–521.
- 25 Purschwitz J, Muller S, Kastner C, Schoser M, Haas H, Espeso EA, Atoui A, Calvo AM and Fischer R (2008) Functional and physical interaction of blue- and red-light sensors in *Aspergillus nidulans*. *Curr Biol* **18**, 255–259.
- 26 Penfold RJ and Pemberton JM (1994) Sequencing, chromosomal inactivation, and functional expression in *Escherichia-Coli* of Ppsr, a gene which represses carotenoid and Bacteriochlorophyll synthesis in Rhodobacter-Sphaeroides. *J Bacteriol* **176**, 2869–2876.
- 27 Jaubert M, Zappa S, Fardoux J, Adriano JM, Hannibal L, Elsen S, Lavergne J, Vermeglio A, Giraud E and Pignol D (2004) Light and redox control of photosynthesis gene expression in Bradyrhizobium: dual roles of two PpsR. *J Biol Chem* **279**, 44407–44416.
- 28 Esteban B, Carrascal M, Abian J and Lamparter T (2005) Light-induced conformational changes of cyanobacterial phytochrome Cph1 probed by limited proteolysis and autophosphorylation. *Biochemistry* **44**, 450–461.
- 29 Lamparter T, Michael N, Mittmann F and Esteban B (2002) Phytochrome from *Agrobacterium tumefaciens* has unusual spectral properties and reveals an N-terminal chromophore attachment site. *Proc Natl Acad Sci USA* **99**, 11628–11633.
- 30 Bhoo SH, Davis SJ, Walker J, Karniol B and Vierstra RD (2001) Bacteriophytochromes are photochromic histidine kinases using a biliverdin chromophore. *Nature* **414**, 776–779.
- 31 Goodner B, Hinkle G, Gattung S, Miller N, Blanchard M, Quorollo B, Goldman BS, Cao Y, Askenazi M, Halling C *et al.* (2001) Genome sequence of the plant

- pathogen and biotechnology agent *Agrobacterium tumefaciens* C58. *Science* **294**, 2323–2328.
- 32 Wood DW, Setubal JC, Kaul R, Monks DE, Kitajima JP, Okura VK, Zhou Y, Chen L, Wood GE, Almeida NF Jr *et al.* (2001) The genome of the natural genetic engineer *Agrobacterium tumefaciens* C58. *Science* **294**, 2317–2323.
  - 33 Karniol B and Vierstra RD (2003) The pair of bacteriophytochromes from *Agrobacterium tumefaciens* are histidine kinases with opposing photobiological properties. *Proc Natl Acad Sci USA* **100**, 2807–2812.
  - 34 Lamparter T, Carrascal M, Michael N, Martinez E, Rottwinkel G and Abian J (2004) The biliverdin chromophore binds covalently to a conserved cysteine residue in the N-terminus of *Agrobacterium phytochrome* Agp1. *Biochemistry* **43**, 3659–3669.
  - 35 Rottwinkel G, Oberpichler I and Lamparter T (2010) Bathy phytochromes in rhizobial soil bacteria. *J Bacteriol* **192**, 5124–5133.
  - 36 Karniol B and Vierstra RD (2004) The HWE histidine kinases, a new family of bacterial two-component sensor kinases with potentially diverse roles in environmental signaling. *J Bacteriol* **186**, 445–453.
  - 37 van Thor JJ, Borucki B, Crielgaard W, Otto H, Lamparter T, Hughes J, Hellingwerf KJ and Heyn MP (2001) Light-induced proton release and proton uptake reactions in the cyanobacterial phytochrome Cph1. *Biochemistry* **40**, 11460–11471.
  - 38 Zienicke B, Molina I, Glenz R, Singer P, Ehmer D, Escobar FV, Hildebrandt P, Diller R and Lamparter T (2013) Unusual spectral properties of bacteriophytochrome Agp2 result from a deprotonation of the chromophore in the red-absorbing form Pr. *J Biol Chem* **288**, 31738–31751.
  - 39 Njimona I and Lamparter T (2011) Temperature effects on *Agrobacterium* phytochrome Agp1. *PLoS ONE* **6**, e25977.
  - 40 Njimona I, Yang R and Lamparter T (2014) Temperature effects on bacterial phytochrome. *PLoS ONE* **9**, e109794.
  - 41 Krieger A, Molina I, Oberpichler I, Michael N and Lamparter T (2008) Spectral properties of phytochrome Agp2 from *Agrobacterium tumefaciens* are specifically modified by a compound of the cell extract. *J Photochem Photobiol, B* **93**, 16–22.
  - 42 Cho H and Winans SC (2007) TraA, TraC and TraD autorepress two divergent quorum-regulated promoters near the transfer origin of the Ti plasmid of *Agrobacterium tumefaciens*. *Mol Microbiol* **63**, 1769–1782.
  - 43 Lamparter T and Michael N (2005) *Agrobacterium* phytochrome as an enzyme for the production of ZZE bilins. *Biochemistry* **44**, 8461–8469.
  - 44 Inomata K, Noack S, Hammam MAS, Khawn H, Kinoshita H, Murata Y, Michael N, Scheerer P, Krauß N and Lamparter T (2006) Assembly of synthetic locked chromophores with *Agrobacterium* phytochromes Agp1 and Agp2. *J Biol Chem* **281**, 28162–28173.
  - 45 McDonagh A (1979) The porphyrins. *Porphyrins* **6**, 243–491.
  - 46 Altmann HJ, Furstena E, Gielewsk A and Scholz L (1971) Photometric determination of small amounts of ortho phosphate with malachite green. *Fresen Z Anal Chem* **256**, 274–275.
  - 47 Kacprzak S, Njimona I, Renz A, Feng J, Reijerse E, Lubitz W, Krauss N, Scheerer P, Nagano S, Lamparter T *et al.* (2017) Intersubunit distances in full-length, dimeric, bacterial phytochrome Agp1, as measured by pulsed electron-electron double resonance (PELDOR) between different spin label positions, remain unchanged upon photoconversion. *J Biol Chem* **292**, 7598–7606.
  - 48 Noack S, Michael N, Rosen R and Lamparter T (2007) Protein conformational changes of *Agrobacterium* phytochrome Agp1 during chromophore assembly and photoconversion. *Biochemistry* **46**, 4164–4176.
  - 49 Immormino RM, Silversmith RE and Bourret RB (2016) A variable active site residue influences the kinetics of response regulator phosphorylation and dephosphorylation. *Biochemistry* **55**, 5595–5609.
  - 50 Fuqua C, Burbea M and Winans SC (1995) Activity of the *Agrobacterium* Ti plasmid conjugal transfer regulator TraR is inhibited by the product of the TraM gene. *J Bacteriol* **177**, 1367–1373.
  - 51 Garcillan-Barcia MP, Francia MV and de la Cruz F (2009) The diversity of conjugative relaxases and its application in plasmid classification. *FEMS Microbiol Rev* **33**, 657–687.
  - 52 Brandt S, von Stetten D, Günther M, Hildebrandt P and Frankenberg-Dinkel N (2008) The fungal phytochrome FphA from *Aspergillus nidulans*. *J Biol Chem* **283**, 34605–34614.
  - 53 Schmidt A, Sauthof L, Szczepek M, Lopez MF, Escobar FV, Qureshi BM, Michael N, Buhrke D, Stevens T, Kwiatkowski D *et al.* (2018) Structural snapshot of a bacterial phytochrome in its functional intermediate state. *Nat Commun* **9**, 4912.
  - 54 Borucki B, Otto H, Rottwinkel G, Hughes J, Heyn MP and Lamparter T (2003) Mechanism of Cph1 phytochrome assembly from stopped-flow kinetics and circular dichroism. *Biochemistry* **42**, 13684–13697.
  - 55 Nagano S, Scheerer P, Zubow K, Michael N, Inomata K, Lamparter T and Krauss N (2016) The crystal structures of the N-terminal photosensory core module of *Agrobacterium* phytochrome Agp1 as parallel and anti-parallel dimers. *J Biol Chem* **291**, 20674–20691.

- 56 Li L, Murphy JT and Lagarias JC (1995) Continuous fluorescence assay of phytochrome assembly *in vitro*. *Biochemistry* **34**, 7923–7930.
- 57 Remberg A, Ruddat A, Braslavsky SE, Gärtner W and Schaffner K (1998) Chromophore incorporation, Pr to Pfr kinetics, and Pfr thermal reversion of recombinant N-terminal fragments of phytochrome A and B chromoproteins. *Biochemistry* **37**, 9983–9990.

## Supporting information

Additional supporting information may be found online in the Supporting Information section at the end of the article.

**Fig. S1.** Coomassie stained SDS/PAGE gels with Agp1 and Agp2 after purification.